

Nuclear dilepton production of Drell-Yan process in the constituent quark model

W. Zhu

Department of Physics, East China Normal University, Shanghai 200062, People's Republic of China

J. G. Shen

Institute of Nuclear Research, Academia Sinica, P. O. Box 800-204, Shanghai 201800, People's Republic of China

(Received 18 July 1990)

The high-mass dilepton production on nuclear targets observed by the E772 Collaboration is analyzed by the constituent quark model. We show that the constituent quark model even without the nuclear shadowing improvement agrees better with the existing data on nuclear targets not only in the inelastic-scattering process, but also in the Drell-Yan process. Further, the QCD improvement for the partonic shadowing model is made. It is found that both the Q^2 dependence of the shadowing strength and the momentum loss due to the annihilation of the shadowed sea quarks evidently depress the distributions of nuclear sea components in the antishadowing region.

I. INTRODUCTION

Recently, the E772 Collaboration¹ at Fermilab published the data of high-mass dilepton production measured in the nuclear Drell-Yan (DY) process.² These data aroused special attention in clarifying the different explanations for the nuclear influence on the momentum distribution of quarks. Their results show that the ratio of DY dimuon yield per nucleon on a nuclear target to that in a free nucleon is slightly less than unity if the momentum fraction x_2 carried by a target quark is less than 0.1. The ratio over the range of $0.1 < x < 0.3$, however, does not reveal distinct nuclear dependence.

Deep-inelastic scattering (DIS) on nuclear targets in the muon and electroproduction processes [i.e., the European Muon Collaboration (EMC) effect] has already shown that the momentum distributions of partons in a nucleon are affected by the nuclear environment. This discovery has provided a large number of different interpretations that describe the DIS equally well. A marked difference of those interpretations is in their distinguishable behavior of nuclear ocean distributions. Bickerstaff, Birse, and Miller³ expected the nuclear DY process to be a valuable tool for sorting them out. The E772 Collaboration made the observations in the kinematic region in which the following quantum chromodynamics (QCD) subprocess is predominant; i.e., a quark from the beam nucleon annihilates with an antiquark from a target nucleon. Their experimental data, to a great extent, just reveal ocean distribution. Therefore, the E772 experiment attaches a peculiar significance to throw light on the origin of the EMC effect.

A series of studies for the nuclear influence on the nucleon structure function were completed by the constituent quark model (CQM).⁴⁻⁹ In this paper we attempt to use the physical picture of the CQM to study the phenomena observed recently in the nuclear DY process. The Q^2 dependence of the nuclear antishadowing is analyzed by perturbative QCD. The organization of the

paper is as follows: We address ourselves to use the CQM to take account into the nuclear DY process in Sec. II. The shadowing improved by QCD are studied in Sec. III. We devoted Sec. IV to analyzing the scaling violations in the shadowing. A conclusion is given in Sec. V.

II. FEATURES OF NAIVE CONSTITUENT QUARK MODEL

What is based on the following consideration for adopting the CQM to analyze the EMC effect?^{4,5} Although the distortion of the current quark distributions is the most remarkable characteristic of the EMC effect, the nuclear effect responsible for the distortion, at the scale of low momentum, acts directly on the wave function of the bound state of a nucleon consisting of the three constituent quarks. It is generally accepted that the constituents (building blocks) of the mesons and baryons appear as a bound system of the type $(q\bar{q})$ or (qqq) , respectively. The point of view successfully describes the low-lying hadron spectrum, the magnetic moments of the baryons, their SU(3) properties, and the F/D ratios of the matrix elements.¹⁰ On the other hand, the weak and electromagnetic currents appear to couple to pointlike objects with quark quantum numbers in the processes with high momentum transfer. Indeed, the probes with high Q^2 in this case "see" those partons dissolved by the constituent quarks and they are called the current quarks or the gluons. These current quarks are not the same as the constituent quarks. So far, the hadron wave function with current quarks is not simply determined by any model at all. The connection between the current quarks and the constituent quarks can be established phenomenologically by a convolution form.^{11,12} To be specific, the sea quark distribution in a free (bound) nucleon $F_{N(A)}^s(x, Q^2)$ can be expressed by the constituent quark distribution $G_{c/N(A)}(y)$ as follows:⁴⁻⁹

$$E_{N(A)}^s(x, Q^2) = \sum_c \int_x^1 dy G_{c/N(A)}(y) F_{c/N(A)}^s(x/y, Q^2), \quad (2.1)$$

where $F_{c/N(A)}^s(z, Q^2)$ is the structure function of the constituent quark in a free (bound) nucleon and has much to do with a probe. The distribution $G_{c/N}$ is distorted by the nuclear interactions to become the distribution $G_{c/A}$.

We assume that the exchange of the wee partons dominates the nuclear interaction, and in whatever form (pionic or other mesonic) the wee partons appear, the three constituent quarks are, on average, "dressed" in them. In this case, as shown in Ref. 9, the probe cannot distinguish between the distribution of the primitive sea quarks in a constituent quark and that of one of the quarks in the mesonic cloud. The structure functions of the constituent quarks are universal and still remain valid in nuclei if nuclear shadowing is neglected, i.e.,

$$F_{c/N}^s(z, Q^2) = F_{c/A}^s(z, Q^2). \quad (2.2)$$

On the other hand, the normalized condition

$$\int_0^1 G_{c/N}(y) dy = \int_0^1 G_{c/A}(y) dy = 1 \quad (2.3)$$

and the momentum sum rule

$$\int_0^1 G_{c/N}(y) y dy = \int_0^1 G_{c/A}(y) y dy = \frac{1}{3} \quad (2.4)$$

for the CQM directly result in the two striking characteristics different from other models. One of them is that incorporated with the normalized condition (2.3), their universality leads to the ratio of the ocean distribution in a bound nucleon to that in a free one:

$$R_{\text{DIS}} = F_A^s(x, Q^2) / F_N^s(x, Q^2), \quad (2.5)$$

to be restricted only to the neighborhood of unity as x approaches zero. It is peculiar to the CQM. Actually, the inconsistency of the original muon production data for the EMC (Ref. 13) from the electroproduction data for the Stanford Linear Accelerator Center¹⁴ (SLAC) arrested our attention in Refs. 4 and 5. According to the characteristic mentioned above, the CQM tends to the SLAC data and, at that time, the CQM is opposite in the ideal to an obvious enhancement of the nuclear ocean components at low x accepted extensively by the other models.¹⁵ Our point was also confirmed by data¹⁶ of Benvenuti *et al.* later. In the sense mentioned above, the CQM provides a good background for describing the other interesting phenomena observed on nuclear targets such as nuclear shadowing, the Drell-Yan pair production, etc.

Another characteristic for the CQM is that, as implied by the sum rule (2.4), their own momenta carried by the ocean quarks and the other components (the valence quarks and the gluons) are preserved, respectively, although the distortion of the distribution $G_{c/A}(y)$ results in the changes of the parton momentum distribution in a bound nucleon. Indeed, associated with the universality for the structure function of the constituent quarks (2.2) and the momentum sum rule (2.4), the formula (2.1) results in

$$\int_0^1 F_N^s(X, Q^2) dx = \int_0^1 F_A^s(x, Q^2) dx$$

and

$$\int_0^1 F_N^v(x, Q^2) dx = \int_0^1 F_A^v(x, Q^2) dx.$$

This implies that the distortion of the constituent quarks immersing in the nuclear environment makes the parton momentum transference restricts only to each parton component itself. Generally speaking, the degraded momenta for the valence quarks in the intermediate region ($0.3 \lesssim x \lesssim 0.7$) of the Bjorken variable x can be transferred into themselves either at low x or at high x .⁶

The DY ratio measured, by the E772 Collaboration¹, is the ratio of the DY differential cross section in nucleon-nucleus scattering to that in nucleon-nucleon scattering:

$$R(x_2) = \frac{\int dx_1 \int dQ^2 d^2\sigma_{N-A}(x_1, x_2, Q^2) / dx_1 dx_2}{\int dx_1 \int dQ^2 d^2\sigma_{N-N}(x_1, x_2, Q^2) / dx_1 dx_2}, \quad (2.6)$$

where the DY cross section per target nucleon is given by²

$$d^2\sigma / dx_1 dx_2 = K \frac{4\pi\alpha^2}{9s} \frac{1}{x_1 x_2} \times \sum_i e_i^2 [q_i(x_1, Q^2) \bar{q}_i(x_2, Q^2) + \bar{q}_i(x_1, Q^2) q_i(x_2, Q^2)]. \quad (2.7)$$

The notations here are presented as follows: α is the fine-structure constant, e_i is the quark (antiquark) charge with the flavor i , \sqrt{s} is the energy in the center-of-mass system, $q_i(x)$ and $\bar{q}_i(x)$ are the quark and antiquark momentum distributions, and K is the QCD correction factor.

In the case of ignoring nucleon shadowing, the DY ratio with the integration range $16 \text{ (GeV}/c)^2 \leq -Q^2 \leq 81 \text{ (GeV}/c)^2$ and $x_1 - x_2 > 0$ are evaluated numerically by the CQM (Refs. 6 and 9) and its result is shown in Fig. 1. It is obvious that the prediction of the CQM is closer to the E772 data by comparison with those of the other models.

In a simple form, the CQM seems to successfully give a reasonable physical picture for the distortion of nuclear structure functions to describe the existing DIS data for the EMC effect, even including the DY data to some extent. In particular, the CQM insisted on considering a few years ago^{4,5} that there was no clear enhancement for nuclear sea quark-antiquark pairs at low x in contrast to most of the other models. This is why the CQM for nuclei can offer a better description for the DY process observed by the E772 Collaboration lately.

III. THE IMPROVEMENT IN THE PARTONIC SHADOWING

Just as the DIS data, the improvements for the nuclear shadowing and antishadowing in the DY process have to be analyzed carefully. In this paper we still employ the improved partonic shadowing model.^{7,9}

The recombination among wee partons in nuclei breaks up the universality of the structure functions for the constituent quarks to give rise to nuclear shadowing. In view of the momentum balance of the quark-parton system, we

have developed the partonic shadowing-antishadowing model in Refs. 7–9. In such a case, the ocean component $F_{A,sa}^s(x, Q^2)$ folded in the nucleon structure function should be expressed by

$$F_{A,sa}^s(x, Q^2) = \begin{cases} \alpha(Q^2)(1-x)^{\beta(Q^2)}, & 0 \leq x \leq x_n, \\ [\alpha(Q^2)(1-x_n)^{\beta(Q^2)}F_A^s(x_n, Q^2)]f(x) + F_A^s(x, Q^2), & x \geq x_n \end{cases} \quad (3.1)$$

with

$$f(x) = \begin{cases} [(1-x/2)/(1-x_n)]^{10}(x_n/x)^2, & x_n \leq x \leq 2x_n, \\ [(1-x/2)/(1-x_n)]^{10}(x_n/2)^2[\frac{3}{2}(2x_n/x)^2(1-2x_n)/(3x)], & x \geq 2x_n. \end{cases} \quad (3.2)$$

Here the point x_n characterizes the occurrence of the onset of shadowing; the subscript *sa* denotes the inclusion of shadowing and antishadowing so as to discriminate it from the sea quark distribution $F_A^s(x, Q^2)$ in a bound nucleon, in which the two effects are not taken into account, and

$$\begin{aligned} \alpha &= F_A^s(0, Q^2)R_s(Q^2), \\ R_s(Q^2) &= 1 - k_s(Q^2)(A^{1/3} - 1) \equiv 1 - k_s(Q^2)n_s. \end{aligned} \quad (3.3)$$

k_s is called the shadowing strength. The power β in the ocean component (3.1) can be determined by the momentum conservation condition

$$\frac{18}{5} \int_0^1 [F_{A,sa}^s(x, Q^2) - F_A^s(x, Q^2)] dx = -n_s \gamma(Q^2), \quad (3.4)$$

where $n_s \gamma(Q^2)$ represents the transference momenta from the ocean to the gluon caused by the recombinations among the shadowed sea quarks.

The experimental condition in the DY process observed by the E772 Collaboration differs from that in the DIS process observed by the EM Collaboration; that is, the $-Q^2$ value of virtual photons in the DY process is far larger than that in the DIS one. As a result, in order to explain the E772 experiment, one should take into account every possibility of Q^2 dependences in theory and their corresponding scaling violations in the shadowing. It is shown in Ref. 6 that, because of the covariance for the Q^2 dependences of the numerator and of the denominator in the DIS ratio (2.5), the Q^2 dependence of the ratio $R_{\mu}(x, Q^2)$ of the structure functions is not obvious in the CQM without the shadowing modification. Now we are devoted to study the Q^2 dependences of the shadowing strength $K_s(Q^2)$ in the formula (3.3) and of the transference factor $\gamma(Q^2)$ in the formula (3.4).

(i) As shown in the DIS process, except that a much smaller part $n_s \gamma(Q^2)$ of the ocean momenta lost in the shadowing region is transferred into the gluons, a great part of it could be compensated in the antishadowing region such that the sea quark distribution over the range $0.1 < x < 0.3$ would evidently be enhanced. In order to calculate the transference factor $n_s \gamma(Q^2)$, one should throw light on the dynamics for the recombination mechanism. The partonic recombination is dominated by a nonperturbative QCD process and, in the meantime, it has a perturbative QCD tail expressed as a nonlinear term. For lack of the knowledge of soft QCD, postponing the details of the recombination dynamics temporarily, it seems appropriate to make a simple presumption that the partonic recombination probability is directly proportional to the partonic density square. The experimental values of the transference momentum square Q^2

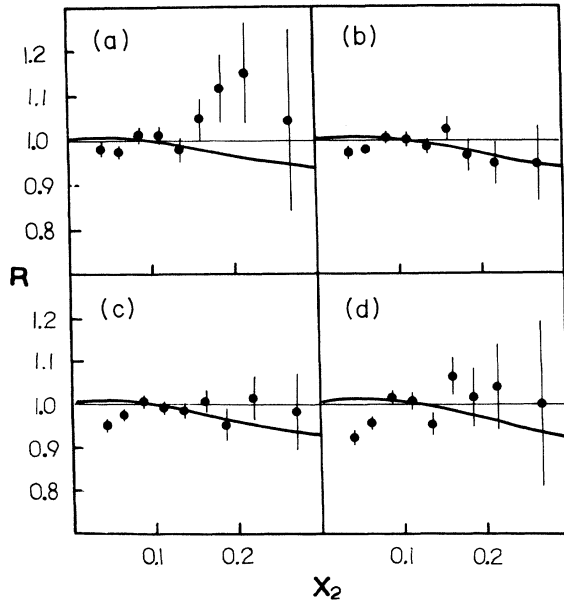


FIG. 1. The prediction of the naive CQM for the ratios of the Drell-Yan dimoun yield in the kinematic region $4 < M_{\mu\mu} < 9$ GeV and $x_1 - x_2 > 0$. (a) C/H, (b) Ca/H, (c) Fe/H, (d) W/H. The data are taken from the E772 experiment (Ref. 1).

for the DIS data are not high in the small- x region, for example, $Q^2 < 20$ (GeV/c)² for $x < 0.1$ in the EMC data. In contrast, the $-Q^2$ values of the E772 data correspond to 16–81 (GeV/c)². According to QCD, the density of

ocean quarks at low x is enhanced with Q^2 increasing. Hence, it can be expected that more momenta are transferred into the gluons by way of the annihilation of the shadowed sea quarks at high Q^2 . So we get

$$\gamma(Q^2) \approx \gamma(Q_c^2) \int_{0.001}^{x_n} x [q_A^s(x, Q^2)]^2 dx / \int_{0.001}^{x_n} x [q_A^s(x, Q_c^2)]^2 dx . \quad (3.5)$$

Here the contribution for $x < 0.001$ was ignored. As for an iron target,⁹ $n_s \gamma(Q_c^2) = 0.0036$ is taken if $Q_c^2 = 10$ (GeV/c)². In this way, $n_s \gamma(Q^2) = 0.0064$ at $Q^2 = 50$ (GeV/c)². What we want to emphasize here are that, on the one hand, the momentum loss of the ocean quarks would depress the ocean distribution in the antishadowing region. Especially in the DY process, such a depression is stronger than that in the DIS process because of the more important role of the ocean quarks relative to the valence quarks here. On the other hand, the momenta lost by the ocean quarks are only a much smaller part of the total momenta originally carried by the ocean quarks. The increase in the ocean momentum loss could be considered as one of the reasons for which the nuclear antishadowing effect in the E772 data is weaker. The DY ratio R for iron is shown by the broken line in Fig. 2 in which the shadowing has already been taken into account, but it is supposed that the shadowing strength $k_s(Q^2) = 0.1$ is independent of Q^2 . As shown by the result, although the antishadowing in the DY process at high Q^2 could be depressed, to some extent, in compar-

ison with that in the DIS process at low Q^2 [see formula (3.5)], the stronger shadowing and antishadowing are still demonstrated by the theoretical result. This implies the existence of another factor depending on Q^2 in a stronger manner.

(ii) Now we proceed to analyze the Q^2 dependence of the shadowing strength $k_s(Q^2)$. The recombination role in the partonic shadowing model reflects on two points. One of them, the nonperturbative recombination effect, could be phenomenologically expressed by the primitive nuclear ocean and gluon distributions, including the shadowing strength $K_s(\mu^2)$ and $K_g(\mu^2)$. Another of them, the perturbative recombination effect, would be expressed as a nonlinear term inversely proportional to Q^2 .

Some of authors considered hitherto that the Q^2 dependence of the partonic shadowing is not obvious. They assumed that the nonlinear tail describing the perturbative parton recombination process is not negligible within the range of available Q^2 for the present experiments. Such a nonlinear term is required to remedy the weakening of the shadowing strength with Q^2 evolving.¹⁷ The observation made by the E772 Collaboration, however, motivated us to study another possibility in contrast to Ref. 17; that is, there exists such a scale Q_c^2 for which the nonlinear term for $Q^2 > Q_c^2$ could be ignored. In this case the modified Altarelli-Parisi equations¹⁷ will be degenerated to the normal QCD evolution equations.¹⁸

If the value of Q^2 is raised from $Q^2 = \mu^2$ to $Q^2 = Q_c^2$, both the shadowing strengths $k_s(Q^2)$ and $k_g(Q^2)$ could be approximately considered as unchanged because of the nonlinear term at work, namely, $k_s(\mu^2) = k_s(Q_c^2)$ and $k_g(\mu^2) = k_g(Q_c^2)$. After this, the shadowing strength for the sea quarks for $Q^2 > Q_c^2$ can be completely deduced by the evolution of the ocean and the gluon shadowing at $Q^2 \sim Q_c^2$ as input for the procedure. Actually, the shadowing of the ocean quarks for $Q^2 > Q_c^2$ is formed by the original ocean shadowing mixed with the ocean shadowing produced by the gluon splitting. The shadowing strength of the latter depends on that for the gluons.

What interests us is whether or not $k_s(\mu^2)$ is equal to $k_g(\mu^2)$. From the point of view of QCD, the sea quarks are directly formed by the gluons, whereas the gluons are primarily produced by the QCD bremsstrahlung of the valence quarks. The nuclear shadowing effect for the ocean quarks comes from two sources: they are either the recombination of the gluons or that of the ocean quarks. But the gluon shadowing is owed to the gluon recombination (there hardly exists shadowing for the valence quarks^{7,9}). It seems that the ocean shadowing

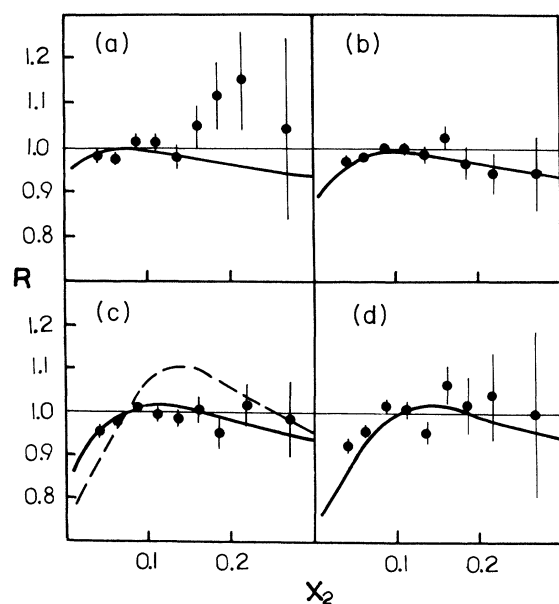


FIG. 2. The same as Fig. 1, except in the CQM with the shadowing improved by QCD. The solid line corresponding to $k_s(Q^2)$ is Q^2 dependent and the broken line corresponding to $K_s(Q^2) = 0.1$ is Q^2 independent.

due to the two sources is stronger than that for the gluons due to the only one and so $k_s(Q_c^2) > k_g(Q_c^2)$ is plausible. A similar conclusion is also made in Ref. 17.

If the conjecture about $k_s(Q_c^2) > k_g(Q_c^2)$ just mentioned is correct, it may be considered that the ocean quarks with Q^2 increasing are continuously compensated by those coming from the weaker gluon shadowing and so such a mixed shadowing would be weakened logarithmically.

It will be shown in the next section that the Altarelli-Parisi equations under the leading-logarithm approximation (LLA) can provide a possible evolution form for the shadowing strength $k_s(Q^2)$ in a simple way.

IV. THE SCALING VIOLATION OF SHADOWING

As shown in Sec. III, the shadowing observation made by the E772 Collaboration is weaker than that made by the EM Collaboration and it could be viewed as the weakening of the ocean shadowing strength $k_s(Q^2)$ with Q^2 evolving. In addition, $k_s(Q_c^2) > k_g(Q_c^2)$ with Q_c^2 being the moderate scale. If $Q^2 > Q_c^2$, the n th-moment equations for the ocean distribution in a constituent quark become¹⁸

$$\begin{aligned} \langle F_{c/N}^s(Q^2) \rangle_n &= \langle F_{c/N}^s(Q_c^2) \rangle_n K_{qq}^n(Q^2) \\ &+ \langle F_{c/N}^g(Q_c^2) \rangle_n K_{qg}^n(Q^2) \\ &+ \langle F_{c/N}^v(Q_c^2) \rangle_n K_{NS}^n(Q^2), \end{aligned} \quad (4.1)$$

$$\begin{aligned} \langle F_{c/A}^s(Q^2) \rangle_n &= \langle F_{c/A}^s(Q_c^2) \rangle_n K_{qq}^n(Q^2) \\ &+ \langle F_{c/A}^g(Q_c^2) \rangle_n K_{qg}^n(Q^2) \\ &+ \langle F_{c/A}^v(Q_c^2) \rangle_n K_{NS}^n(Q^2), \end{aligned} \quad (4.2)$$

where $\langle F(Q^2) \rangle_n \equiv \int_0^1 z^{n-2} F(z, Q^2) dz$ and the nuclear shadowing do not affect the distributions of valence quarks in the constituent quarks. The definition of each quantity in Eqs. (4.1) and (4.2) is given in the Appendix.

In view of the Regge asymptotic behaviors of the gluons and of the ocean quarks as x tends to zero, their distribution in a free nucleon can be taken as the Buras-Caemers forms:¹⁹

$$\begin{aligned} F_{c/N}^s(z, Q^2) &= a_N^s(Q^2)(1-z)^{b_N^s(Q^2)}, \\ F_{c/N}^g(z, Q_c^2) &= a_N^g(Q_c^2)(1-z)^{b_N^g(Q_c^2)}, \\ F_{c/N}^s(z, Q_c^2) &= a_N^s(Q_c^2)(1-z)^{b_N^s(Q_c^2)}, \end{aligned} \quad (4.3)$$

where the subscripts s and g are corresponding to the sea quark distribution and the gluon one, respectively. Moreover, the shape of formula (4.3) would evidently be changed by the parton recombination. In analogy to formulas (3.1) and (3.3), the nuclear parton distribution effect of the nuclear shadowing effect could be written as

$$\begin{aligned} F_{c/A}^s(z, Q^2) &= R_s(Q^2) a_N^s(Q^2) (1-z)^{b_A^s(Q^2)} \\ &\equiv a_A^s(Q^2) (1-z)^{b_A^s(Q^2)}, \\ F_{c/A}^g(z, Q_c^2) &= R_g(Q_c^2) a_N^g(Q_c^2) (1-z)^{b_A^g(Q_c^2)} \\ &\equiv a_A^g(Q_c^2) (1-z)^{b_A^g(Q_c^2)}, \\ F_{c/A}^s(z, Q_c^2) &= R_s(Q_c^2) a_N^s(Q_c^2) (1-z)^{b_A^s(Q_c^2)} \\ &\equiv a_A^s(Q_c^2) (1-z)^{b_A^s(Q_c^2)}. \end{aligned} \quad (4.4)$$

Here the shadowing effect reflects on $a_A^s(Q^2) < a_N^s(Q^2)$ and $a_A^g(Q_c^2) < a_N^g(Q_c^2)$ as well as $a_A^s(Q_c^2) < a_N^s(Q_c^2)$. One of the characteristics of the CQM without the shadowing improvement is that the distortion of the constituent quark distributions immersing in the nuclear environment does not change the average momenta of all the parton components. Although the antishadowing strength is affected by the momentum transference from the sea quarks to the gluons in the shadowing process, the momenta transferred are only a much smaller part of the total momenta carried originally by the ocean quarks and, in general, it is estimated to be $\sim 4\%$ if $Q^2 = 50$ (GeV/c)². If the momentum loss owing to the recombination process of the shadowed ocean quarks is negligible, the momenta carried by each parton component would be conserved separately and approximately,

$$\begin{aligned} \langle F_{c/N}^s(Q^2) \rangle_2 &\equiv \langle F_{c/A}^s(Q^2) \rangle_2, \\ \langle F_{c/N}^g(Q^2) \rangle_2 &\equiv \langle F_{c/A}^g(Q^2) \rangle_2, \end{aligned} \quad (4.5)$$

and the following inequalities will be satisfied for $Q^2 > \mu^2$:

$$\langle F_{c/N(A)}^{s(g)}(Q^2) \rangle_2 \gg \langle F_{c/N(A)}^{s(g)}(Q^2) \rangle_3. \quad (4.6)$$

As a result, we acquire

$$\begin{aligned} R_s(Q^2) &= 1 - k_s(Q^2)(A^{1/3} - 1) \\ &= \lim_{x \rightarrow 0} \frac{F_A^s(x, Q^2)}{F_N^s(x, Q^2)} = \frac{a_A^s(Q^2)}{a_N^s(Q^2)} \approx \frac{\langle F_{c/N}^s(Q^2) \rangle_3}{\langle F_{c/A}^s(Q^2) \rangle_3}, \end{aligned} \quad (4.7)$$

$$\begin{aligned} R_s(Q_c^2) &= 1 - k_s(Q_c^2)(A^{1/3} - 1) \\ &= \lim_{x \rightarrow 0} \frac{F_A^s(x, Q_c^2)}{F_N^s(x, Q_c^2)} = \frac{a_A^s(Q_c^2)}{a_N^s(Q_c^2)} \approx \frac{\langle F_{c/N}^s(Q_c^2) \rangle_3}{\langle F_{c/A}^s(Q_c^2) \rangle_3}, \end{aligned} \quad (4.8)$$

$$\begin{aligned} R_g(Q_c^2) &= 1 - k_g(Q_c^2)(A^{1/3} - 1) \\ &= \lim_{x \rightarrow 0} \frac{F_A^g(x, Q_c^2)}{F_N^g(x, Q_c^2)} = \frac{a_A^g(Q_c^2)}{a_N^g(Q_c^2)} \approx \frac{\langle F_{c/N}^g(Q_c^2) \rangle_3}{\langle F_{c/A}^g(Q_c^2) \rangle_3}. \end{aligned} \quad (4.9)$$

Suppose that $R_s(Q_c^2) = \lambda R_g(Q_c^2)$ with $\lambda < 1$. This implies that the primitive shadowing for the gluon distribution is weaker than that for the ocean distribution. We acquire

$$\begin{aligned}
R_s(Q^2) &= \frac{\langle F_{c/N}^s(Q_c^2) \rangle_3 K_{qq}^3(Q^2) + \langle F_{c/N}^g(Q_c^2) \rangle_3 K_{qg}^3(Q^2) + \langle F_{c/N}^v(Q_c^2) \rangle_3 K_{Ns}^3(Q^2)}{\langle F_{c/A}^s(Q_c^2) \rangle_3 K_{qq}^3(Q^2) + \langle F_{c/A}^g(Q_c^2) \rangle_3 K_{qg}^3(Q^2) + \langle F_{c/N}^v(Q_c^2) \rangle_3 K_{Ns}^3(Q^2)} \\
&= R_s(Q_c^2) \frac{\langle F_{c/N}^s(Q_c^2) \rangle_3 K_{qq}^3(Q^2) + \langle F_{c/N}^g(Q_c^2) \rangle_3 K_{qg}^3(Q^2) + \langle F_{c/N}^v(Q_c^2) \rangle_3 K_{Ns}^3(Q^2)}{\langle F_{c/N}^s(Q_c^2) \rangle_3 K_{qq}^3(Q^2) + \lambda \langle F_{c/N}^g(Q_c^2) \rangle_3 K_{qg}^3(Q^2) + R_s(Q_c^2) \langle F_{c/N}^v(Q_c^2) \rangle_3 K_{Ns}^3(Q^2)}. \quad (4.10)
\end{aligned}$$

It turns out that the evolution of $R_s(Q^2)$ with Q^2 depended on λ and Q_c^2 . Moreover, $R_g(Q^2)$ is larger than that of the sea quarks ($\lambda < 1$). In this case, the shadowing strength $k_s(Q^2)$ would be correspondingly degraded with Q^2 increasing. The magnitude in its change also depends on Q_c^2 . As a matter of fact, the QCD evolution of the parton distribution depends entirely on

$$L = \ln(Q^2/\Lambda^2)/\ln(Q_c^2/\Lambda^2).$$

The smaller Q_c^2 is, the larger the quantity L taken by the same value of Q^2 becomes. For lack of the information about the primitive parton distributions in the nuclear medium and about the nonperturbative dynamics for the recombination process, we are unable to determine the values of λ and Q_c^2 theoretically. However, it is plausible to extract their values from the fitting of the E772 data. Then the k_s value at low Q^2 determined by the QCD evolution process is compared with the data measured by the EM Collaboration²⁰ and the others. To this end, some sets of values of λ and Q_c^2 are chosen to calculate formula (4.10). Their results are plotted in Fig. 3 with $k_s(Q_c^2)=0.1$ and $k_g(Q_c^2)=0.05$, in which $Q_c^2=10$ (GeV/c)², $Q_c^2=4$ (GeV/c)², and $Q_c^2=1$ are shown by the solid line, the broken one, and the dotted-broken one, respectively. In comparison with the E772 experiment, it is found that

$$k_s(Q^2=50 \text{ (GeV/c)}^2) = 0.06$$

is an appropriate choice. It corresponds to $Q_c^2 \sim 1$ GeV/c². This implies that it is unnecessary to modify the Altarelli-Parisi equations by adding the nonlinear term within the available range of Q^2 for the present experiments. This conclusion differs from Ref. 17.

Taking formula (3.5) into account, formula (4.10) can be calculated by the CQM and its result is shown by the solid line with

$$k_s(Q^2 \sim 50 \text{ (GeV/c)}^2) = 0.06$$

in Fig. 2, which is also consistent with the E772 data.

Since the QCD evolution equations under the LLA is unsuitable for the case of low Q^2 , the change of the strength k_s only for $Q^2 > 10$ (GeV/c)² is shown in Fig. 3. But we could estimate that the variations from $k_s(Q_c^2)=0.1$ to

$$k_s(Q^2=10 \text{ (GeV/c)}^2) \approx 0.07$$

are smoothly connected to each other. This indicates the evident weakening of the strength $k_s(Q^2)$ in the region

$$1 \text{ (GeV/c)}^2 < Q^2 < 10 \text{ (GeV/c)}^2.$$

As Q^2 is continuously increased from $Q^2=10$ (GeV/c)²,

the strength $k_s(Q^2)$ slowly tends to its limit value $k_g(Q_c^2)$. In order to judge whether the behavior about the evident weakening of $k_s(Q^2)$ at the scale of low Q^2 contradicts the existing DIS data, we use the approach mentioned above to evaluate the DIS ratio of the structure functions once again. Its calculations on a calcium target are plotted in Fig. 4, where the solid line and the broken one, as well as the dashed one, represent $Q_c^2=1, 10$, and 40 (GeV/c)², respectively. As shown by Fig. 4, there exists the scaling violation in the low- x region ($x < 0.01$) and the antishadowing region ($x \sim 0.15$). The DIS data at different Q^2 values measured by the EM Collaboration²⁰ are plotted in Fig. 4 where a lack of the DIS data at high Q^2 for $x < 0.1$ is truly a pity. Here we illustrate the scaling violation in the DIS ratio within the antishadowing region ($x \sim 0.15$) in Fig. 5 with the data taken from the Benvenuti *et al.* Collaboration.²¹ What we stress here is that the scaling violation in the shadowing expected by our approach is consistent with the available DIS experimental data. Of course, the further observation about the nuclear DIS process at different Q^2 for $x < 0.01$ or $x \sim 0.15$ will be helpful to test our theory.

Since the shadowing strength $k_s(Q^2)$ in the shadowing formula (3.3) exerts influence on the ocean distribution in the form of $[1 - k_s(Q^2)(A^{1/3} - 1)]$, it may be expected that the scaling violation due to the change of $k_s(Q^2)$ is revealed by heavy nuclei more remarkably.

V. CONCLUSION

In a simple form, the CQM for nuclei offers a physical picture of the distortion for nucleon structure function entering the nuclear surrounding. This model sheds light on some useful ideas such as the nuclear medium affects the distribution of the constituent quarks in a bound nucleon rather than the structure functions of the constituent quarks. The momentum conservation of each parton component remains approximately valid in the nuclear medium. In particular, it is emphasized as the universality

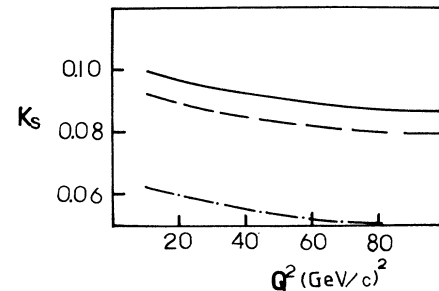


FIG. 3. The Q^2 dependence of shadowing strength $k_s(Q^2)$. $k_s(Q_c^2)=0.1$ and $k_g(Q_c^2)=0.05$ are taken here. The solid and broken lines, as well as the dotted-broken one represent $Q_c^2=10, 4$, and 1 (GeV/c)², respectively.

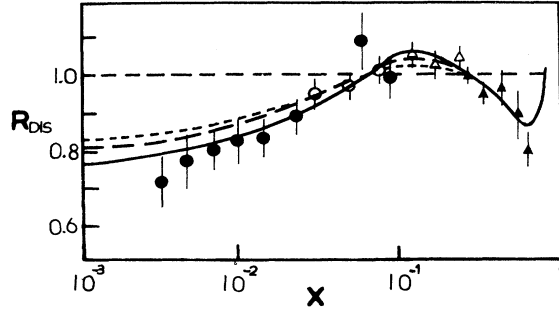


FIG. 4. The model prediction of the scaling violation in the nuclear shadowing for the DIS on a calcium target. The solid line and the broken one, as well as the dotted one, correspond to $Q^2=1, 10,$ and 40 (GeV/c)^2 , respectively. The data marked by the black circle, the white circle, the white triangle, and the black triangle represent $Q^2 \sim 1, 10, 20,$ and 40 (GeV/c)^2 , respectively. The vertical axis is the ratio R_{DIS} of the structure functions with $R_{\text{DIS}} = F_2(\text{Ca})/F_2(\text{D})$.

ty of the constituent quarks. The implication behind the universality is that it never has any striking enhancement in nuclear wee partons at low x . Such behavior of nuclear quark-antiquark pairs in the CQM provides a good background for both the DIS data and the DY data.

Within the framework of the CQM for nuclei, the Q^2 dependence of the partonic shadowing process is carefully analyzed. The shadowing strength k_s for the nuclear ocean extracted from the E772 data has much to do with the Q^2 dependence. These variation rule can be explained by the Altarelli-Parisi evolution equations. Moreover, it does not contradict the existing EMC, SLAC, and Benvenuti *et al.* data.

The CQM incorporated with the improved partonic shadowing mechanism gives the following distortion picture of the quark momentum distribution immersing in the nuclear environment: Parts of the momenta carried by the ocean are transferred into themselves from the

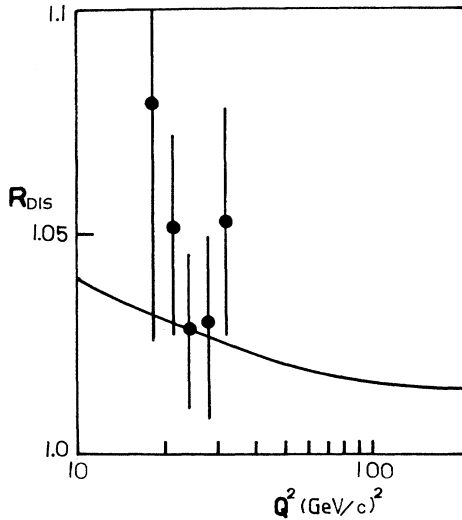


FIG. 5. The model prediction of the scaling violation in the nuclear antishadowing for the DIS on an iron target. The vertical axis represents the ratio R_{DIS} of the structure function with $x=0.15$. The data came from Ref. 21.

shadowing region ($x < 0.1$) to the antishadowing region ($x \sim 0.15$). In the meantime, a much smaller part of the total momenta carried by the ocean is transferred into the gluons. Another point we would like to make is that the distortion of the valence quarks is dominated by their momentum transference from the intermediate x region to themselves either at low x ($x < 0.3$) or at high ($x > 0.7$).

Because of the depression of the shadowing strength as well as the enhancement of the momentum loss of the ocean quarks in the DY process at high Q^2 observed by the E772 Collaboration, the phenomenon of the quark enhancement in the antishadowing region ($0.1 < x < 0.3$) nearly disappears.

It could be expected that (i) A more evident scaling violation either in the shadowing region ($x < 0.01$) or in the antishadowing region ($x \sim 0.15$) would be observed if the Q^2 of the DIS probe on heavy nuclear targets changes from 1 (GeV/c)^2 to about 10 (GeV/c)^2 , (ii) a stronger antishadowing effect would be observed if the dilepton mass produced by the nuclear DY process becomes smaller, and (iii) the shadowing of the gluons is weaker than that of the ocean quarks.

In summary, the high-mass dilepton production on nuclear targets observed by the E772 Collaboration is analyzed by the constituent quark model. It shows that the CQM, even without the shadowing improvement, agrees better with the existing data not only in the DIS process but also in the DY process. Further, the QCD improvement for the partonic shadowing model is made. It is found that both the Q^2 dependence of the shadowing strength and the momentum loss due to the annihilation of the shadowed ocean quarks evidently depress the distributions of nuclear ocean components in the antishadowing region.

We would like to acknowledge support in part for this research from the China National Science Foundation.

APPENDIX

The quantities of Eqs. (3.6) and (3.7) are (see Ref. 18)

$$\begin{aligned}
 K_{qq}^n(Q^2) &= a_n L^{-a_n^-} + (1 - \alpha_n) L^{-a_n^+}, \\
 K_{qg}^n(Q^2) &= \beta_n (L^{-a_n^-} - L^{-a_n^+}), \\
 K_{Ns}^n(Q^2) &= [\alpha_n L^{-a_n^-} + (1 - \alpha_n) L^{-a_n^+} - L^{-a_{Ns}^n}], \\
 L &= \ln(Q^2/\Lambda^2) / \ln(Q_c^2/\Lambda^2), \\
 a_n^\pm &= (P_{qq}^n - P_{qg}^n + \Delta) / 2P_{qg}^n, \\
 \Delta &= [(P_{gg}^n - P_{qq}^n)^2 + 4P_{qg}^n P_{qg}^n]^{1/2}, \\
 P_{qq}^n &= C_F \left[-\frac{1}{2} + 1/n(n+1) - 2 \sum_2^n 1/j \right], \\
 2fP_{qg}^n &= f(2+n+n^2)/n(n+1)(n+2), \\
 P_{qg}^n &= C_F(2+n+n^2)/n(n^2-1), \\
 P_{gg}^n &= 2C_A \left[-\frac{1}{12} + 1/n(n-1) \right. \\
 &\quad \left. + 1/(n+1)(n+2) - \sum_2^n 1/j \right] - f/3.
 \end{aligned}$$

- ¹D. M. Alde *et al.*, Phys. Rev. Lett. **64**, 2479 (1990).
²S. D. Drell and T. M. Yan, Phys. Lett. **25**, 316 (1970).
³R. P. Bickerstaff, M. C. Birse, and G. A. Miller, Phys. Rev. Lett. **53**, 2523 (1984).
⁴W. Zhu, Commun. Theor. Phys. **3**, 565 (1984); W. Zhu, J. G. Shen, and X. J. Qiu, Phys. Lett. **154B**, 20 (1985).
⁵C. H. Chang and W. Zhu, Phys. Lett. B **187**, 405 (1987).
⁶W. Zhu and J. G. Shen, Phys. Lett. B **219**, 107 (1989).
⁷W. Zhu and J. G. Shen, Phys. Lett. B **235**, 170 (1990).
⁸W. Zhu and J. G. Shen, J. Phys. G **16**, 925 (1990).
⁹W. Zhu and J. G. Shen, Phys. Rev. C **41**, 1674 (1990).
¹⁰H. J. Lipkin, Nucl. Phys. **A446**, 409c (1985).
¹¹G. Altarelli, N. Cabibbo, L. Maiani, and R. Petronzio, Nucl. Phys. **B69**, 531 (1974); V. V. Anisovich, Phys. Lett. **57B**, 87 (1975).
¹²R. C. Hwa, Phys. Rev. D **22**, 759 (1980); **22**, 1593 (1980).
¹³J. Aubert *et al.*, Phys. Lett. **123B**, 275 (1983).
¹⁴A. Bodek *et al.*, Phys. Rev. Lett. **50**, 1431 (1983).
¹⁵D. Von Harrach, Nucl. Phys. **A478**, 290 (1988).
¹⁶A. C. Benvenuti *et al.*, Phys. Lett. B **189**, 483 (1987).
¹⁷A. H. Mueller and J. Qiu, Nucl. Phys. **B268**, 427 (1986); J. Qiu, *ibid.* **B291**, 746 (1987).
¹⁸G. Altarelli and G. Parisi, Nucl. Phys. **B126**, 298 (1977).
¹⁹A. J. Guras and J. K. F. Gaemers, Nucl. Phys. **B132**, 249 (1978).
²⁰The EM Collaboration, J. Ashman *et al.*, Phys. Lett. B **202**, 603 (1988); **211**, 493 (1988).
²¹The BCDMS Collaboration, A. C. Benvenuti *et al.*, Phys. Lett. B **189**, 483 (1987).